Spatial representation of organic carbon and active-layer thickness of high latitude soils in CMIP5 earth system models

Umakant Mishra [a,*], Beth Drewniak [a], Julie D. Jastrow [a], Roser M. Matamala [a], U.W.A. Vitharana [b]

[a] Environmental Science Division, Argonne National Laboratory, 9700 South Cass Avenue, Argonne, IL 60439, USA
[b] Department of Soil Science, University of Peradeniya, 20400 Peradeniya, Sri Lanka

ARTICLE INFO

ABSTRACT

Soil properties such as soil organic carbon (SOC) stocks and active-layer thickness are used in earth system models (ESMs) to predict anthropogenic and climatic impacts on soil carbon dynamics, future changes in atmospheric greenhouse gas concentrations, and associated climate changes in the permafrost regions. Accurate representation of spatial and vertical distribution of these soil properties in ESMs is a prerequisite for reducing existing uncertainty in predicting carbon-climate feedbacks. We compared the spatial representation of SOC stocks and active-layer thicknesses predicted by the coupled Model Intercomparison Project Phase 5 (CMIP5) ESMs with those predicted from geospatial predictions, based on observation data for the state of Alaska, USA. For the geospatial modeling, we used soil profile observations (585 for SOC stocks and 153 for active-layer thickness) and environmental variables (climate, topography, land cover, and surficial geology types) and generated fine-resolution (50-m spatial resolution) predictions of SOC stocks (to 1-m depth) and active-layer thickness across Alaska. We found large inter-quartile range (2.5–5.5 m) in predicted active-layer thickness of CMIP5 modeled results and small inter-quartile range (11.5–22 kg m^{-2}) in predicted SOC stocks. The spatial coefficient of variability of active-layer thickness and SOC stocks were lower in CMIP5 predictions compared to our geospatial estimates when gridded at similar spatial resolutions (24.7 compared to 30% and 29 compared to 38%, respectively). However, prediction errors, when calculated for independent validation sites, were several times larger in ESM predictions compared to geospatial predictions. Primary factors leading to observed differences were (1) lack of spatial heterogeneity in ESM predictions, (2) differences in assumptions concerning environmental controls, and (3) the absence of pedogenic processes in ESM model structures. Our results suggest that efforts to incorporate these factors in ESMs should reduce current uncertainties associated with ESM predictions of carbon-climate feedbacks.

1. Introduction

The spatial heterogeneity of terrestrial land surfaces affects energy, moisture, and greenhouse gas exchanges with the atmosphere. However, representing heterogeneity of soil properties and processes in earth system models (ESMs) remains a critical scientific challenge (Mishra and Riley, 2015). ESMs use soil properties such as soil organic carbon (SOC) stocks and active-layer (AL) thickness to predict carbon-climate feedbacks of permafrost affected regions. In permafrost affected soils, AL is the top portion of soil column that freezes and thaws with seasonal temperature changes in winter and summer (Zhang et al., 2005). The AL thickness or depth is measured as the maximum depth of thaw in any particular year. Accurate representation of spatial and vertical heterogeneity of these soil properties in ESMs is a prerequisite

for reducing existing uncertainty in predicting carbon-climate feedbacks (Burke et al., 2012; Todd-Brown et al., 2013).

Perennially frozen soils of the northern circumpolar region store the largest quantity of SOC in the terrestrial biosphere (Tarnocai et al., 2009; Hugelius et al., 2014), primarily due to processes like cryoturbation, peat formation, and sedimentation of windblown and waterborne silt particles (e.g., Ping et al., 1998; Tarnocai and Stolbovoy, 2006; Schirrmeister et al., 2011; Ping et al., 2011; and Strauss et al., 2012). Anticipated increase in atmospheric temperature of these regions may cause widespread permafrost thaw leading to remobilization of previously frozen SOC pools (Schuur and Abbott, 2011; Ping et al., 2015). Consequent releases of greenhouse gases could cause a positive feedback to Earth's atmosphere resulting into further warming (Schaefer et al., 2011). At present, substantial difference exists between observation based SOC stock estimates and ESM baseline SOC stock estimates that are used in predicting future carbon-climate feedbacks (Mishra et al., 2013). As the soil carbon dynamics due to land use and climate change depend mainly on the magnitude of baseline SOC (Bellamy et al., 2005; Todd-Brown et al.,

* Corresponding author.
  E-mail address: umishra@anl.gov (U. Mishra).

2013), ESMs predict very large ranges in SOC losses from permafrost under future warming scenarios (25–85 Pg C by 2100) which results in large uncertainty for predicting carbon-climate feedbacks from climate warming in the permafrost regions (Koven et al., 2011).

Active-layer thicknesses of permafrost affected land surface determines the volume of SOC susceptible to decomposition and thermal erosion, and are being used in ESMs to predict carbon-climate feedbacks of permafrost regions (Koven et al., 2013a). The surface temperature increases have been linked to increased AL thickness and decreased permafrost extent (Zhang et al., 2005; Jorgenson et al., 2010). Permafrost temperatures have increased in most regions since the early 1980s, and the observed warming was between 2 and 3 °C in parts of the Northern circumpolar region from 1971 to 2010. By 2100, the global mean temperature could increase by 2.6–4.8 °C (IPCC, 2013). The extent and thickness of permafrost at high northern latitudes will be reduced in response to the global mean surface temperature increases. By the end of the 21st century, the extent of the land area containing shallow permafrost (permafrost found in the upper 3.5 m of the soil profile) is projected to decrease between 37% (RCP2.6) to 81% (RCP8.5) (IPCC, 2013). The increase in temperature predicted by 2100 in high-latitude regions could deepen the AL thickness, thereby moving SOC into the AL where it may become more susceptible to microbial decomposition and thermal erosion.

Earth system models are used to predict the response of land surface (including arctic ecosystems) under future climate change. By integrating vegetation and surface energy balance with soil properties (e.g. texture) and processes (e.g. SOC turn over), ESMs can estimate the carbon-climate feedbacks under future warming at global scales. Recent earth system modeling studies (Lawrence and Slater, 2005; Schaefer et al., 2011; MacDougall et al., 2012; Schneider von Deimling et al., 2012; Koven et al., 2013a) have predicted spatial variability of SOC stocks and AL thickness across Alaska and the Northern Hemisphere at coarse spatial resolutions (>100 km), and have demonstrated large variability between models. Therefore, the Coupled (i.e., interactive two-way coupling between the land and atmosphere) Model Intercomparison Project Phase 5 (CMIP5) model simulation experiments were designed to examine and compare the behavior of state-of-the-art ESMs (Taylor et al., 2009; Reichstein et al., 2013). The results from these CMIP5 models are being used in the current Intergovernmental Panel on Climate Change (IPCC) fifth assessment report. At present large uncertainties exist in predicting carbon-climate feedbacks of permafrost regions using these ESMs (IPCC, 2013; Fisher et al., 2014). Among other factors distribution of SOC stocks and AL thickness contribute to a significant portion of the predicted uncertainty (Burke et al., 2012; Koven et al., 2013a). Therefore, there is a critical need to create observation based geospatial datasets that is consistent with the existing landscape heterogeneity and use them as benchmarks to constrain model projections, provide quantitative errors on these estimates, and improve upon the existing mechanisms represented in ESMs.

In this study, our objective was to evaluate the spatial representation of SOC stocks and AL thickness that are being used to predict the carbon climate feedbacks in current CMIP5 ESMs. Specific objectives were to (i) generate fine-resolution (50-m) estimates of SOC stocks and AL thickness across Alaska using soil profile observations and secondary information of soil forming factors (environmental factors), and (ii) compare the spatial heterogeneity representations in these predictions with those projected in the CMIP5 ESMs.

2. Materials and methods

2.1. Study area, soil profile observations, and environmental datasets

We chose the state of Alaska, USA, for this study as this part of the northern circumpolar permafrost region has the highest data intensity (both soil observations and environmental datasets). We used 585 georeferenced soil profile observations from a recently published database (Michaelson et al., 2013) to predict the SOC stocks to 1-m depth (Fig. 1a). This database updated the USDA-National Cooperative Soil Survey data for Alaska and combined it with data collected by the University of Alaska Fairbanks Northern Latitudes Soils Program from 1991 through 2011. In this database, 153 samples reported AL thickness (Fig. 1c). Out of 153, AL thickness of 59 samples were measured by digging soil profiles and measuring the depth to the permanently frozen portion of the soil profile, and in the other 94 samples AL thickness was calculated as depth to soil horizons with permanently frozen layers as indicated by 'f' suffix, such as Cf, Cgf, and Bgf (Mishra and Riley, 2012, 2014; Ping et al., 2013; Soil Survey Staff, 2014) of the soil profile.

We used a digital elevation model of 50-m spatial resolution from the U.S. Geological Survey (USGS) database (Gesch et al., 2009). The elevation of the study area ranged from sea level to 6188 m. High-elevation areas are located in the southeastern part of Alaska, and low-elevation areas are located in the western and northern parts of Alaska. We derived several primary and secondary topographic attributes and evaluated their use in predicting SOC stocks and AL thickness. These topographic attributes included elevation, slope, aspect, curvature (plan, profile, and total), upslope contributing area, flow length, soil wetness index, sediment transport index, stream power index, terrain characterization index, and slope aspect index (Thompson et al., 2006). Land cover data of 60-m spatial resolution were extracted for Alaska from the National Land Cover Database (Homer et al., 2007). We reclassified the NLCD land cover types into nine major categories. The largest land area was under the scrub (shrub < 5 m tall) category (43%), followed by forest (25%), barren (8.5%), herbaceous (7%), and wetlands (7%). The remaining surface area (9.5%) was under open water, perennial ice, cultivated, and developed categories. Long–term climate data (1961–1990) for average annual temperature, precipitation, potential evapotranspiration (PET), and summer shortwave radiation were obtained from the Scenario Network for Alaska and Arctic Planning (SNAP, 2014) database. Across Alaska the mean annual air temperature and mean annual precipitation ranged from −18 °C to 6 °C and 150 mm to 8500 mm, respectively. Average annual (1981–2000) net primary productivity data was collected from the Global Land Cover Facility of University of Maryland database (Prince and Goward, 1995). The surface geology data of Alaska was obtained from a USGS database (Karlstrom, 1964; scale 1:1,584,000) in which the entire state of Alaska was classified into 27 different types of surficial geology. The category with the largest land area was mountain alluvium and colluvium (22.5%), followed by coarse rubble (19%), coastal alluvium (8.5%), glacial moraine (7%), and undifferentiated mosaics (6%). The remaining land area (37%) was placed in the remaining 22 surficial geology types. Indicator variables for the presence or absence of land cover types and surficial geology were created and used in the model selection process. All the environmental datasets were resampled to a common spatial resolution of 50 m by using the resample function of ArcGIS (ArcGIS version 10, Environmental Systems Research Institute, Inc., Redlands, CA, USA).

2.2. Geospatial predictions of SOC stocks and active-layer thickness

Several spatial prediction techniques exist in soil science literature (Minasny et al., 2013). We chose geographically weighted regression (GWR) approach for this study as this approach is relatively easy to implement and has been reported to produce better or similar prediction accuracy in comparison to other prediction techniques such as ordinary least square regression, inverse distance weighted, ordinary kriging, and regression kriging (Mishra et al., 2010; Zhang et al., 2011). Further GWR approach allowed us to evaluate environmental controls of investigated soil properties which changes across space in a large study area like ours. We used best subset regression in SAS 9.3 (SAS Institute, 2011) to generate all possible combinations of environmental controllers to predict both the SOC stocks and AL thickness across Alaska. First, we used Mallows' Cp criterion to select three candidate linear models for each soil property for which Cp values were close to the number of predictors (Kutner et al.,
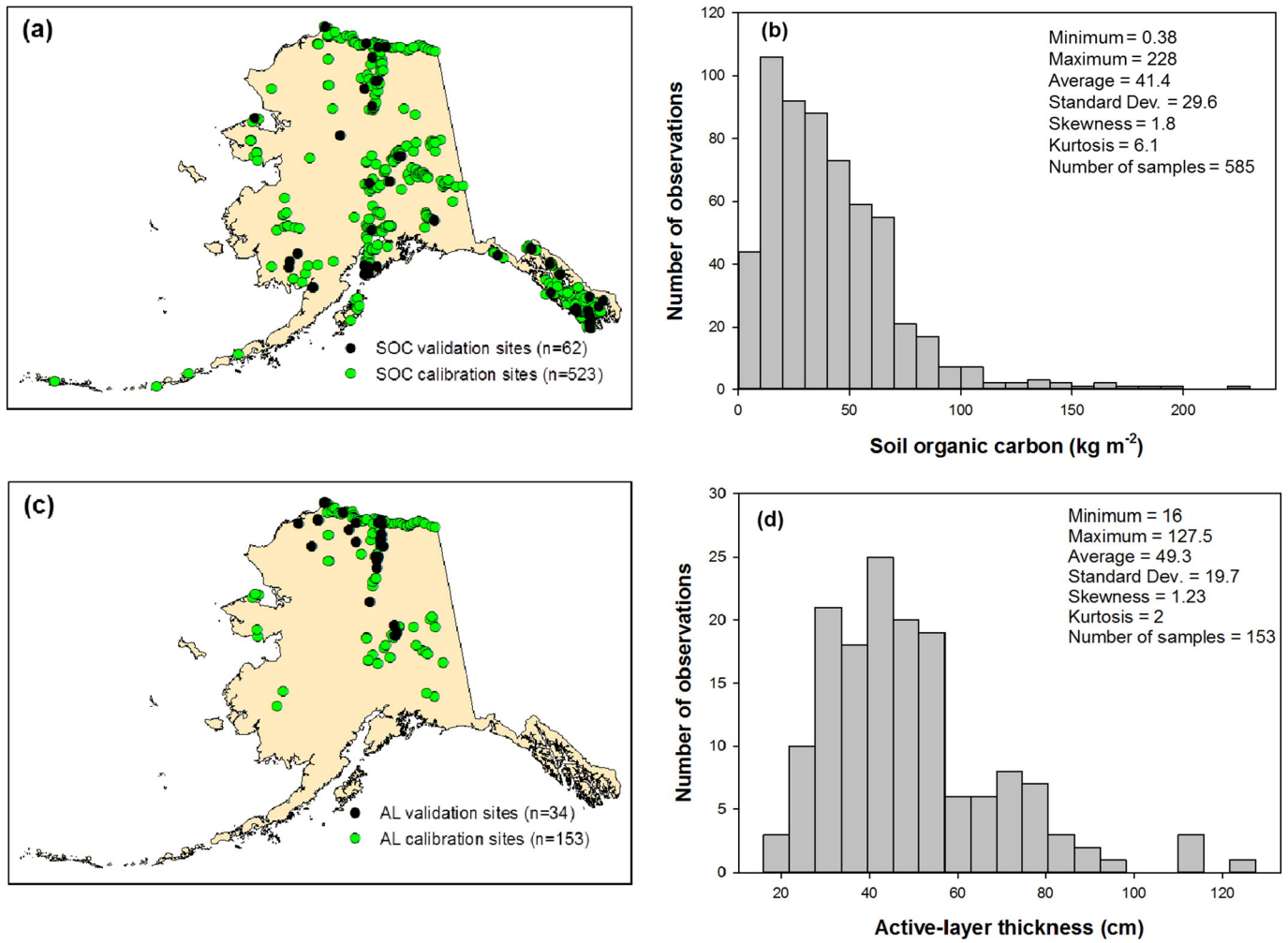
Fig. 1. Spatial and statistical distributions of soil organic carbon (SOC) stock (a, b), and active-layer (AL) thickness (c, d) samples across Alaska.

2004; p. 358). Next, we selected one of the candidate linear models for each SOC stock and AL thickness with uncorrelated and statistically significant environmental predictors. The selected environmental predictors were then used in a geographically weighted regression (GWR) approach (Mishra and Riley, 2012, 2014) to predict the soil properties across Alaska:

$$S(u_i, v_i) = \beta_o(u_i, v_i) + \sum_{i=1}^{p} \beta_k(u_i, v_i) X_k + \varepsilon(u_i, v_i)$$

where S is the soil property at a certain location, u_i, v_i are the geographical coordinates, X_k are the environmental predictors, p is the number of independent variables, β_o and β_k are the geographically weighted regression coefficients, and ε is the error term. We used adaptive kernel

bandwidth in this study, given that the sample density varied over the study area. The optimal bandwidth was determined by minimizing the corrected Akaike Information Criterion (AICc) as described in Fotheringham et al. (2002). Table 1 shows the fitted geographically weighted regression model summary for log transformed SOC stocks to 1-m depth interval. We used the results of Mishra and Riley (2014) for AL thickness because no new samples of AL thickness were available to us to conduct a new analysis.

2.3. Spatial uncertainty estimation

We used an empirical approach of uncertainty estimation to generate spatially heterogeneous estimates of uncertainty for SOC stocks

Table 1
Geographically weighted regression model summary for log-transformed soil organic carbon stocks to 1-m depth (model calibration $R^2 = 0.10$–0.48).

Predictor	Minimum	Lower quartile	Median	Upper quartile	Maximum
Intercept	2.60	2.65	2.72	2.84	3.42
Elevation	−0.00067	−0.00063	−0.00053	−0.00040	−0.00011
Aspect	0.00020	0.00040	0.00060	0.00072	0.00097
Temperature	−0.10	−0.099	−0.081	−0.031	−0.015
Potential evapotranspiration	0.028	0.068	0.112	0.135	0.15
Mountain alluvium & colluvium	0.088	0.14	0.20	0.26	0.49
Barren land cover	−2.36	−0.63	−0.60	−0.58	−0.51

and AL thickness predictions. In this approach, the residuals between modeled outputs and corresponding observed values of model calibration data were used to generate prediction intervals (Shrestha and Solomatine, 2006; Malone et al., 2011). Environmental covariates were partitioned into n clusters using fuzzy k-means clustering algorithm (Minasny and McBratney, 2002). For SOC stocks, the environmental covariates include elevation, aspect, temperature, potential evapotranspiration, land cover type, and surficial geology; and mean surface air temperature, land cover type, and slope gradient were the environmental covariates used in clustering for AL thickness. In order to find the optimal values for the number of clusters and fuzziness exponent values, the fuzzy k-means clustering was performed iteratively with a cluster size of 2 through 10, and the resulting fuzziness performance index and the normalization classification entropy values were observed. The class number that minimizes fuzziness performance index and normalization classification entropy was considered optimum (Odeh et al., 1992). The fuzziness exponent value was set for 1.35 as suggested by Odeh et al. (1992). The optimal cluster size for the given environmental was found to be 5, for both SOC stocks and AL thickness.

After identifying the clusters that each calibration site belongs on the basis of highest membership value, the lower and upper prediction intervals (PIC_i^L and PIC_i^U, respectively) for each cluster were computed from empirical distributions of residuals within each cluster. To generate 95% prediction interval for each cluster we used lower 2.5% and upper 97.5% percentile values from the empirical distribution of residuals in each cluster. The following procedure of Shrestha and Solomatine (2006) was followed to calculate the upper and lower prediction interval of each location:

$$PI_i^L = \sum_{j=1}^{c} m_{ij} PIC_j^L$$

$$PI_i^U = \sum_{j=1}^{c} m_{ij} PIC_j^U$$

where PI_i^L and PI_i^U are the weighted lower and upper prediction intervals for the i-th observation, PIC_j^L and PIC_j^U are the lower and upper prediction intervals for the j-th cluster, and m_{ij} the membership grade of i-th observation to cluster j. The lower and upper prediction limits were then estimated for each observation by using following equations:

$$PL_i^L = Pr_i + PI_i^L$$

$$PL_i^U = Pr_i + PI_i^U$$

where PL_i^L and PL_i^U are the lower and upper prediction limits of the i-th observation, respectively, and Pr_i is the model prediction at the i-th observation.

For ESM predictions, we generated uncertainty estimates (95% confidence intervals) by using four ESM model predictions (Table 2).

2.4. Comparing observation-based predictions with ESM predictions

We compared geospatial predictions of SOC stocks and AL thickness distribution across Alaska with predictions from four coupled ESMs that

contributed to the CMIP5 database (Taylor et al., 2009). We chose four ESMs that captured the range of spatial resolutions of ESM projections (158–295 km): Japan Agency for Marine-Earth Science and Technology (MIROC-ESM; 158 km), Geophysical Fluid Dynamics Laboratory Earth System Model with GOLD Ocean Component (GFDL-ESM2G; 184 km), Canadian Earth System Model version 2 (CanESM2; 211 km), and Beijing Climate Center Climate System Model version 1-1 (BCC-CSM1-1; 295 km) (Table 2).

For comparison between observation-based and the CMIP5 ESM predictions, we calculated several statistical parameters of soil properties such as median, inter-quartile range, and coefficient of variability, from both observation-based and CMIP5 ESM predictions. We also evaluated prediction accuracy of both GWR and ESM predictions using 62 independent validation sites for SOC stocks and 34 sites for AL thickness obtained from the circumpolar AL monitoring network data (Brown et al., 2000; CALM, 2013) data. Predicted values of SOC stocks and AL thickness were extracted at validation sites from both GWR and ESM predictions and interpreted by calculating mean estimation error (MEE), root mean square error (RMSE), and ratio of performance to deviation values (Chang and Laird, 2002). Chang and Laird (2002) defined three classes of ratio of performance to deviation; models that have high predictive ability (ratio of performance to deviation > 2), models that have intermediate predictive ability which can be possibly improved (ratio of performance to deviation between 1.4 and 2), and models that have no predictive ability (ratio of performance to deviation < 1.4). Comparisons of coefficient of variability of soil properties were made by gridding the predicted soil properties at the same spatial resolutions as that of generated by ESM predictions.

3. Results

3.1. Descriptive statistics of observations

The average SOC stock to 1-m depth across 585 samples was 41.4 kg m^{-2}, ranging from 0.38 to 228 kg m^{-2}. The SOC stocks showed unimodal (kurtosis = 6.1), and a positively skewed (skewness = 1.8) distribution (Fig. 1b). Majority of SOC samples (69% samples) showed SOC stocks <50 kg m^{-2}, about 4% samples had >100 kg m^{-2}, and rest (~27%) had SOC stocks in between 50 and 100 kg m^{-2}. High observed SOC stocks were found in forest, wetlands, and herbaceous land cover types. These observations were associated with low elevation (32–<200 m), and high potential evapotranspiration values (>12 mm day^{-1}). Low observed SOC stocks were found in barren, scrub, and cultivated land cover types. These observations were associated with high elevation (200–1500 m) and low potential evapotranspiration values (0.5–<10 mm day^{-1}).

The average AL thickness across the 153 permafrost samples was 0.49 m, ranging from 0.16 to 1.27 m. AL thickness showed unimodal (kurtosis = 2), and close to normal distribution (coefficient of skewness = 1.23) (Fig. 1d). Out of all AL thickness observations, 54% of samples showed <0.5 m AL thickness, 4 samples had >1 m AL thickness, and rest (~42%) showed 0.5–1 m Al thickness. Low AL thickness observations were found in low elevation (<30 m) and in herbaceous and wetland land cover types. High AL thickness observations were located in relatively higher elevation (>150 m), and in barren, forest, and scrub land cover types. Though the samples were unequally distributed

Table 2
Four Coupled Model Intercomparison Project Phase 5 (CMIP5) earth system model outputs and their soil properties used for comparison across Alaska.

Models	Average AL thickness (m)	Average SOC stocks (kg m^{-2})	Spatial resolution (km)	Modeling groups	References
BCC-CSM1-1	3.36 ± 0.4	8.4 ± 2	295	Beijing Climate Center	Ji, 1995
CanESM2	3.9 ± 0.8	32 ± 8.8	211	Canadian Earth System Model	Verseghy, 1991
GFDL-ESM2G	3.9 ± 4.4	12.3 ± 3.5	131	Geophysical Fluid Dynamics Laboratory	Dunne et al., 2012
MIROC-ESM	12 ± 4.6	20.5 ± 9.8	158	Japan Agency for Marine-Earth Science and Technology	Takata et al., 2003

Table 3
Geographically weighted regression predicted average and coefficient of variability (CV) of active-layer thickness and soil organic carbon (SOC) stocks across different ecoregions of Alaska.

Ecoregions	Average active-layer thickness	CV active-layer thickness	Average SOC stocks	CV SOC stocks
Bering Taiga	48.0	35.8	28.6	11.7
Aleutian Meadows	0.0		29.0	26.7
Alaska Range Transition	40.0	47.7	21.0	31.6
Coastal Rainforests	0.0		32.0	48.0
Arctic Tundra	28.3	28.5	36.3	34.1
Bering Tundra	44.2	10.2	30.6	14.9
Pacific Mountain Transition	52.5	5.6	20.4	13.6
Intermontane Boreal	47.8	13.6	24.0	16.1
Coastal Mountain Transition	42.2	20.8	15.2	40.2

through Alaska, they captured a wide range of environmental heterogeneity including; all 27 major land resource areas, and all soil taxonomic units (18) of Alaska at soil suborder level.

3.2. Spatial heterogeneity of predicted SOC stocks and active-layer thickness

Predicted SOC stocks to 1-m depth showed high spatial variability (coefficient of variability = 41%), ranging from 2 to 72 kg m^{-2} with an average across Alaska of 28 kg m^{-2}. We are 95% confident that the true average Alaska SOC stock is between 26 and 30 kg m^{-2}. Among different ecoregions, Arctic Tundra showed highest amount of SOC stocks (36 kg m^{-2}, with lower and upper prediction intervals of 34 and 38 kg m^{-2} respectively), followed by Coastal Rainforests (32 kg m^{-2}, with lower and upper prediction intervals of 31 and 34 kg m^{-2} respectively), and Bering Tundra (30 kg m^{-2}, with lower and upper prediction intervals of 28 and 32 kg m^{-2} respectively). Aleutian Meadows and Bering Taiga had similar levels of average SOC stocks (~29 kg m^{-2}, with

lower and upper prediction intervals of 27 and 30 kg m^{-2} respectively). Lowest amount of SOC stocks (15 kg m^{-2}, with lower and upper prediction intervals of 13 and 17 kg m^{-2} respectively) were predicted in Coastal Mountain Transition ecoregion (Table 3). On average our approach under-predicted Alaskan SOC stocks by 6 kg m^{-2} (MEE = −6 kg m^{-2}). The average prediction error (RMSE) was 27 kg m^{-2}, and the observed ratio of performance to deviation was 1.2, indicating our approach has a moderate predictive ability for SOC stocks (Chang and Laird, 2002; Gomez et al., 2008). The validation data showed that our approach predicted 47% of the observed variance of Alaskan SOC stocks (model validation R^2 = 0.47). Higher prediction errors were primarily due to our approach substantially under-predicting the observed SOC stocks at 7 validation sites having SOC stocks >100 kg m^{-2}. Our approach predicted less than half of the observed SOC stocks at these sites.

The predicted average AL thickness across Alaska was 0.46 m, ranging from 0.14–0.93 m. We are 95% confident that the true average
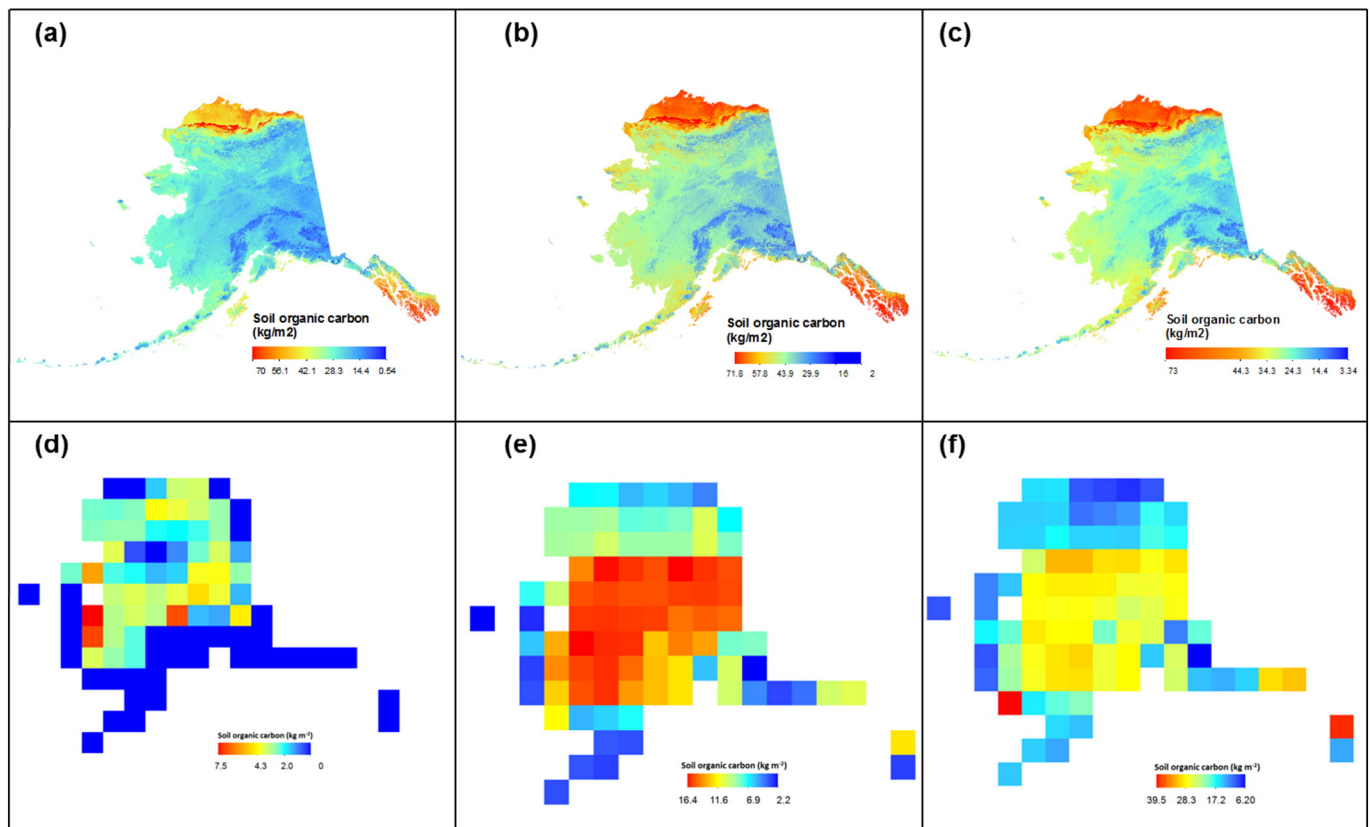

Fig. 2. Spatial distribution of soil organic carbon stocks to 1-m depth predicted by geographically weighted regression approach (b) with its lower (a) and upper (c) prediction intervals in comparison to average SOC stock represented in four CMIP5 ESMs (e) with its lower (d) and upper (f) confidence intervals.

Alaska AL thickness is between 0.42 and 0.49 m. Consistent with expectations the average AL thickness increased from north to south with the lowest values at Arctic Tundra (0.28 m, with lower and upper prediction intervals of 0.26 and 0.30 m respectively), and the highest values at Pacific Mountain Transition and lowlands of the Bering Taiga ecoregion (Table 3). On an average our approach under-predicted the AL thickness by 3.6 cm (MEE = −0.036 m). The average error of AL thickness prediction (RMSE) compared to the CALM observations was 0.11 m, and the observed ratio of performance to deviation of predicted map was 1.8. These global validation indices showed good prediction accuracy for AL thickness across the state (Chang and Laird, 2002). Among different ecoregions, lowest AL thickness was found in Arctic Tundra, followed by Alaska Range Transition (0.40 m, with lower and upper prediction intervals of 0.26 and 0.30 m respectively), and Coastal Mountain Transition (0.42 m). Intermontane Boreal and Bering Taiga had similar AL thickness (~0.48 m, with lower and upper prediction intervals of 0.47 and 0.49 m respectively), and highest AL thickness (0.53 m, with lower and upper prediction intervals of 0.50 and 0.55 m respectively) was predicted in Pacific Mountain Transition ecoregion.

3.3. Comparing spatial heterogeneity and prediction accuracy of soil properties with CMIP5 ESM predictions

The average coefficient of variability of SOC stocks represented in ESM predictions was 30% in comparison to 38% in GWR prediction when gridded at same spatial resolutions. The average interquartile range of SOC stocks across ESM models ranged from 11.5–22 kg m^{-2} with a median of 19.7 kg m^{-2} (Fig. 2d,e,f). Where as in GWR predictions, the interquartile range of SOC stocks was 22.2–31.6 with a median of 26.7 kg m^{-2} (Fig. 2a,b,c). The ESM models under-predicted Alaskan SOC stocks (MEE = −25.5 kg m^{-2}) in comparison to GWR prediction

(MEE = −6 kg m^{-2}).The average error of prediction (RMSE) was substantially higher in ESM predictions (42 kg m^{-2}) in comparison to GWR prediction (27 kg m^{-2}). The overall predictive ability of SOC stocks was low (ratio of performance to deviation = 0.71) in ESMs compared to the moderate predictive ability of GWR predicted map (ratio of performance to deviation = 1.2).

The average interquartile range of AL thickness across CMIP5 ESM model predictions ranged from 2.5 to 5.5 m, with a median of 5 m (Fig. 3d,e,f). In GWR prediction, the median AL thickness was 0.45 m and the interquartile range was 0.35 to 0.56 m (Fig. 3a,b,c). The average coefficient of variability of AL thickness in ESM predictions was 24.7% compared to 30% in GWR predictions when gridded at same spatial resolutions. The prediction errors were substantially higher in ESM predictions. Across Alaska, CMIP5 models over-predicted AL thickness by 4.6 m (MEE = 4.6 m). The average error of prediction was 5 m (RMSE = 5 m), and the ratio of performance to deviation was 0.28. In contrast, GWR results under-predicted AL thickness by 0.04 m (MEE = −0.04 m), and the average prediction error across Alaska was 0.11 m. Likewise, the RPD was 1.8, an indicative of good prediction accuracy.

4. Discussion

Our estimates of SOC stocks are comparable to previous estimates of Alaskan carbon stocks. For example, Ping et al. (2008) reported Arctic SOC stocks to 1-m depth interval to be 35 kg m^{-2} in comparison to our estimate of 36 kg m^{-2}. Johnson et al. (2011) reported average SOC stocks to 1-m depth of 44 kg m^{-2}, 14 kg m^{-2}, 26 kg m^{-2}, and 25 kg m^{-2} for Arctic Tundra, Intermontane Boreal, Alaska Range Transition, and coastal rainforest ecoregions, respectively. In a recent northern circumpolar
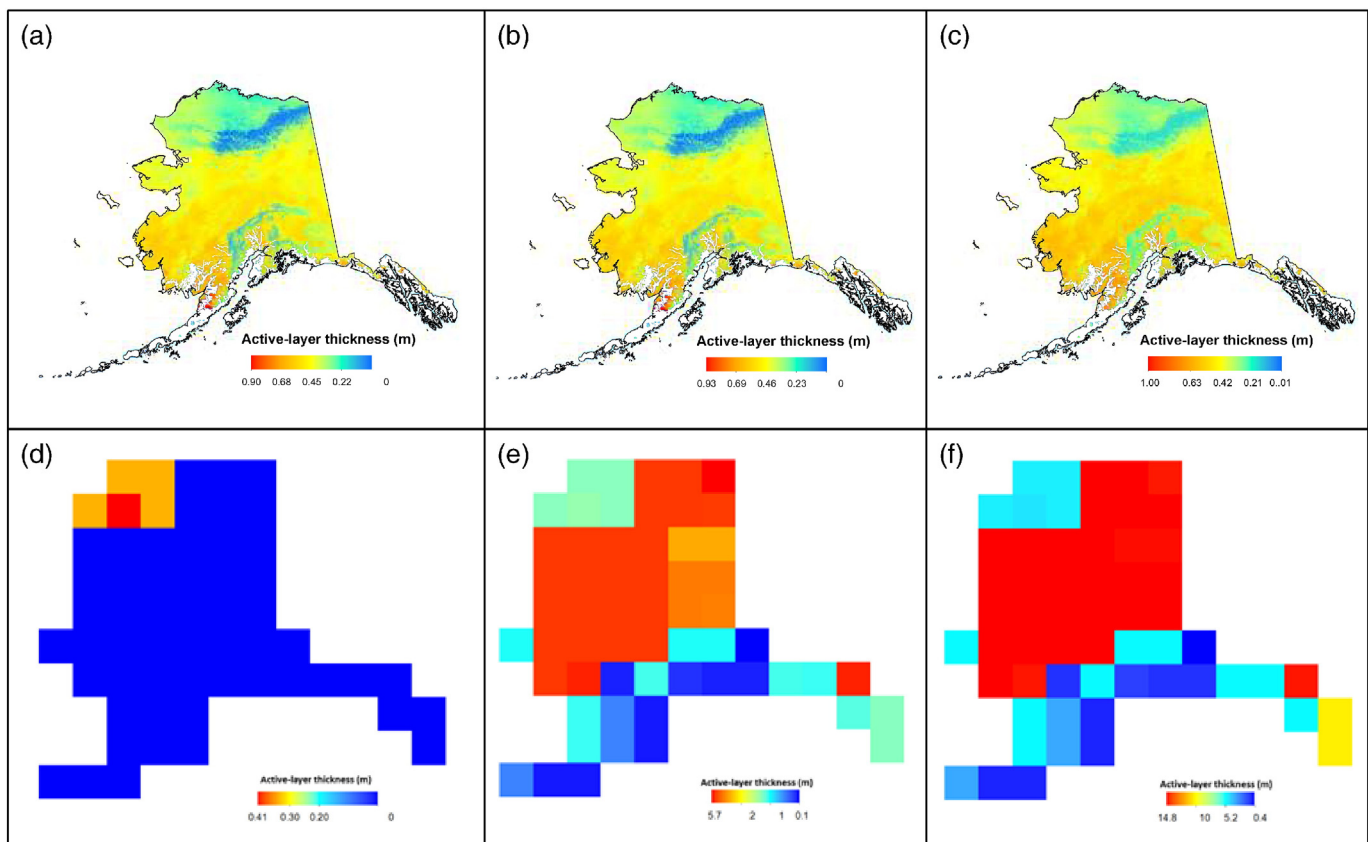

Fig. 3. Spatial distribution of active-layer thickness (b; adopted from Mishra and Riley, 2014) with its lower (a) and upper (c) prediction intervals in comparison to average active-layer thickness represented in four CMIP5 ESMs (e) with its lower (d) and upper (f) confidence intervals. Areas in white show no active-layer thickness.

study, Hugelius et al. (2014) reported average Alaskan SOC stocks of 21 kg m^{-2} in comparison to our estimate of 28 kg m^{-2}. Hugelius et al. (2014) reported SOC stocks of 32 kg m^{-2}, 18 kg m^{-2}, and 17 kg m^{-2} in Arctic Tundra, Intermontane Boreal, and Alaska Range Transition ecoregions respectively. Our estimates are within the range of these previous estimates.

In this study, we did not intend to compare various spatial prediction techniques. GWR approach that we used allowed us to investigate spatially variable environmental controls in our study area. We observed modest predictive capability of generated maps of SOC stocks and AL thickness (ratio of performance to deviation = 1.2 for SOC stocks and 1.8 for AL thickness) against the validation data (which were not used in the model development), therefore we consider the GWR predicted soil properties presented in this study to be a first step in the development of our method which will benefit from more observations as they become available across the topographic, edaphic, and climatic gradients across Alaska and northern circumpolar region. As the sampling density increases, GWR models could be calibrated at smaller spatial scales

across the study area which could increase our ability to better represent the spatial variability. Predictive performance of GWR approach can be improved when the influences of various arctic environmental controllers on soil properties are better understood. Lower predicted coefficient of variability (36% for SOC stocks and 30% for AL thickness) in comparison to the observed values (71% for SOC stocks and 62% for AL thickness) likely indicate the impact of other environmental factors not included in our analysis, such as cryopedogenic features (Ping et al., 2015) specific to permafrost region soils (e.g., high and low centered polygons, pingos, frost boils), organic layer thickness (Pastick et al., 2014), and fire intensity and variability (Hu et al., 2010). Geospatial datasets of these potentially important factors are not currently available now, so we could not use them in our spatial prediction approach. Their use in geospatial predictions of soil properties should be evaluated once they become available. Problems of local multicollinearity might be observed when there is a large area with the same value of independent categorical variable (Zhang et al., 2011). Some environmental relationships may appear to
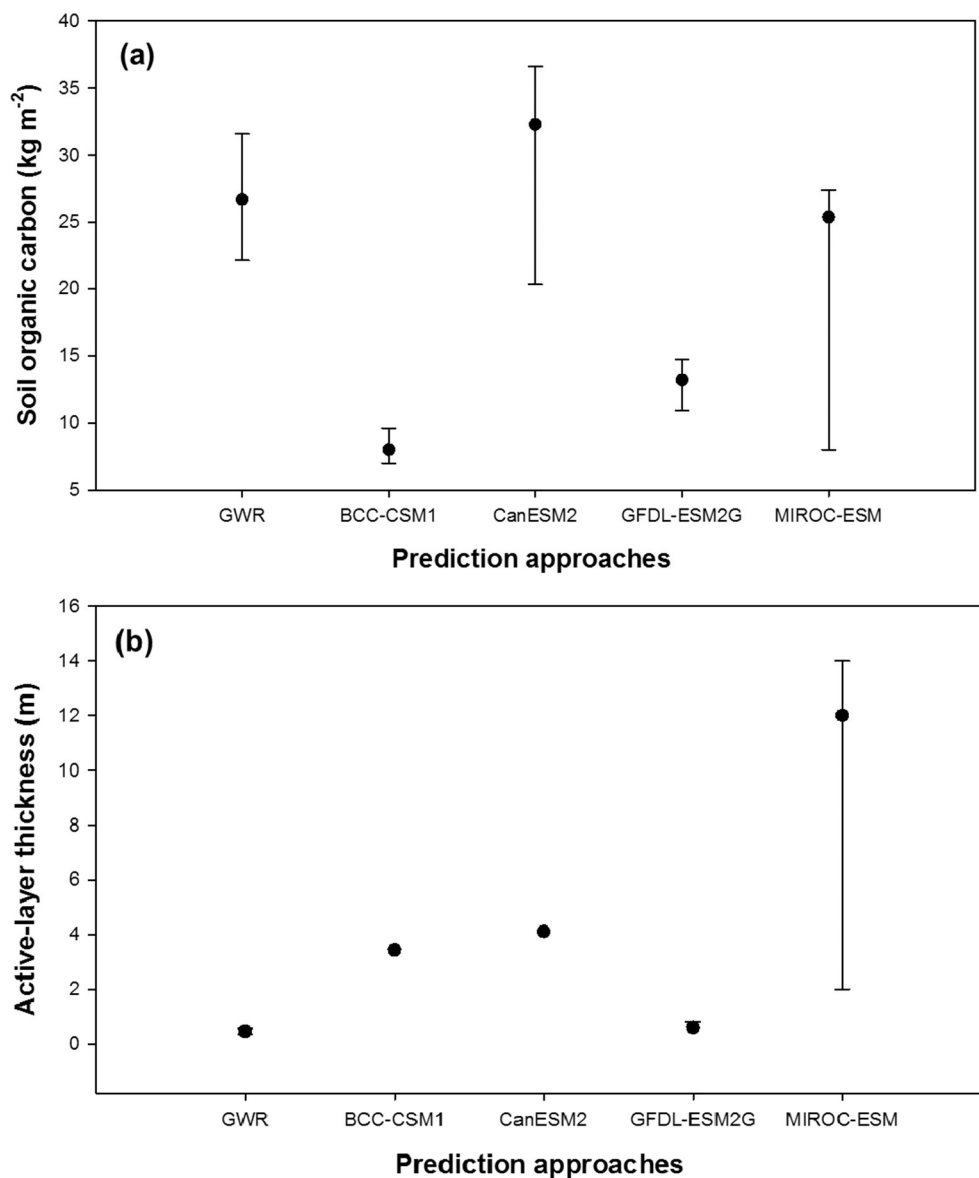

Fig. 4. Observation-based GWR predictions of soil organic carbon stocks (a) and active-layer thickness (b) compared to four CMIP5 ESM predictions across Alaska. Black dot represents median predictions and error bars represent inter-quartile range.

vary locally due to missing variables or interaction between different environmental variables which are not accounted in this approach (Jetz et al., 2005).

The CMIP5 ESM predictions we evaluated in this study show that the SOC stocks increased from north to south across Alaska. These results showed opposite trend in SOC stocks variability of what we predicted using GWR approach (Fig. 2a). One reason behind ESM predictions could be that they predict SOC stocks as a function of net primary productivity (Todd-Brown et al., 2013), which is not consistent with observations from Alaska. Our results suggest other environmental factors such as elevation, aspect, temperature, potential evapotranspiration, land cover type, and surficial geology were predictors of SOC stocks, and net primary productivity was not a statistically significant predictor of SOC stocks across Alaska. Our results demonstrate that the SOC stocks of Alaskan soils can't be predicted using current levels of net primary productivity as the permafrost affected soils are not in equilibrium with current levels of net primary productivity and respiration rates (Mishra et al., 2013). We observed different patterns in AL thickness representation in ESM results. Of the ESM results evaluated in this study, BCC-CSM1, CanESM2, and MIROC-ESM had only two values across Alaska. The GFDL-ESM2G results showed greater variability and the median value of the modeled result was closer to our observed results (Fig. 3b).

Our results suggest current ESMs substantially over-predict current AL thickness and under-predict SOC stocks across Alaska. Both observations are indicative of potential biases in predicting future carbon-climate feedbacks. For example, higher AL thickness indicates higher volume of SOC susceptible of microbial decomposition and thermal erosion. Similarly, lower SOC stock estimates in ESMs are indicative of potentially low greenhouse gas emissions under future warming scenarios. The geospatial approaches used in this study considered the impacts of surface air temperature, land cover types, and topographic attributes to predict AL thickness, and temperature, land cover types, topographic attributes, and surficial geology to predict SOC stocks. Current land models of ESMs use net primary productivity and respiration to predict SOC stocks (Todd-Brown et al., 2013), similarly ESMs use mean annual air temperature as the primary controller of AL thickness (Koven et al., 2013a). Our results suggest ESMs should include additional arctic processes and better model parameterizations such that they can incorporate environmental controls driving active layer thickness (e.g. depth and timing of snowmelt, ice content, microtopography, priming effects, soil mineralization, land cover change, and organic matter thermal insulation) that are responsible for permafrost thaw and SOC turnover to make ESM predictions consistent with the observations.

ESMs are not only increasing in spatial resolution, but many are also starting to include subgrid spatial heterogeneity that can capture small scale variations in carbon and nitrogen cycling, hydrology, vegetation, and radiation. For example, modeling approaches that resolve hydrologic flow around arctic polygons are available (Pau et al., 2014) for ESMs. In addition, with several arctic field campaigns increasing the quantity and quality of available data, focus on model development to improve representation and processes governing arctic ecosystems has increased significantly. For example, the century-type vertical profile of carbon and nitrogen cycling added to community land model (Koven et al., 2013b) substantially improved the carbon storage in arctic ecosystems in community land model. Explicit microbial representation has increased SOC storage in community land model (Wieder et al., 2013), despite these efforts, the spatial heterogeneity representation has not improved. With the advancement in model development, as ESMs come closer to accurately simulating carbon cycle feedbacks in the arctic, our geospatial approach can help model development as a target to guide model activities and encompassing

new data as it becomes available ensuring an accurate benchmark of SOC stocks and AL thickness (see Fig. 4).

5. Summary and conclusions

Projections of soil properties (AL thickness and SOC stocks) by CMIP5 Earth system models had lower coefficients of variation, different range, and larger prediction errors compared to geospatial predictions. Mean surface air temperature, land cover type, and slope gradient were primary controllers of active-layer thickness spatial variability (Mishra and Riley, 2014). Environmental controllers of SOC stocks were topographic attributes, temperature, potential evapotranspiration, land cover, and surficial geology. Primary factors leading to observed differences in spatial heterogeneity and prediction errors between ESMs and geospatial predictions were differences in assumptions concerning environmental controls, lack of spatial heterogeneity in ESM predictions, and the absence of pedogenic processes in ESM model structures. As ESM resolution increases and important ecosystem processes are added to include critical soil dynamics in the arctic, our study provides a spatial benchmark to evaluate ESM outputs of permafrost affected systems. This could potentially help to reduce uncertainties and improve the capability of models to predict carbon-climate feedbacks of permafrost systems.

References

Bellamy, P.H., Loveland, P.J., Bradley, R.I., Lark, R.M., Kirk, G.J.D., 2005. Carbon losses from all soils across England and Wales 1978–2003. Nature 437, 245–248.

Brown, J., Hinkel, K., Nelson, F., 2000. The Circumpolar Active Layer Monitoring (CALM): research designs and initial results. Polar Geogr. 24, 165–258.

Burke, E.J., Hartley, I.P., Jones, C.D., 2012. Uncertainties in the global temperature change caused by carbon release from permafrost thawing. Cryosphere 6, 1063–1076.

Chang, C.W., Laird, D.A., 2002. Near-infrared reflectance spectroscopic analysis of soil C and N. Soil Sci. 167, 110–116.

Dunne, J.P., John, J.G., Adcroft, A.J., Griffies, S.M., Hallberg, R.W., Shevliakova, E., Stouffer, R.J., Cooke, W., Dunne, K.A., Harrison, M.J., Krasting, J.P., Malyshev, S.L., Milly, P.C.D., Phillips, P.J., Sentman, L.T., Samuels, B.L., Spelman, M.J., Winton, M., Wittenberg, A.T., Zadeh, N., 2012. GFDL's ESM2 global coupled climate–carbon earth system models. Part I: Physical formulation and baseline simulation characteristics. J. Clim. 25, 6646–6665.

Fisher, J.B., Sikka, M., Oechel, W.C., Huntzinger, D.N., Melton, J.R., Koven, C.D., Ahlström, A., Arain, M.A., Baker, I., Chen, J.M., Ciais, P., Davidson, C., Dietze, M., El-Masri, B., Hayes, D., Huntingford, C., Jain, A.K., Levy, P.E., Lomas, M.R., Poulter, B., Price, D., Sahoo, A.K., Schaefer, K., Tian, H., Tomelleri, E., Verbeeck, H., Viovy, N., Wania, R., Zeng, N., Miller, C.E., 2014. Carbon cycle uncertainty in the Alaskan Arctic. Biogeosciences 11, 4271–4288.

Fotheringham, A.S., Brunsdon, C., Charlton, M., 2002. Geographically Weighted Regression: the Analysis of Spatially Varying Relationships. John Wiley & Sons Ltd., Chichester, UK.

Gesch, D., Evans, G., Mauck, J., Hutchinson, J., Carswell Jr., W.J., 2009. The National Map—Elevation: U.S. Geological Survey Fact Sheet 2009-3053.

Gomez, C., Rossel, R.A.V., McBratney, A.B., 2008. Soil organic carbon prediction by hyperspectral remote sensing and field vis-NIR spectroscopy: an Australian case study. Geoderma 146, 403–411.

Homer, C., Dewitz, J., Fry, J., Coan, M., Hossain, N., Larson, C., Herold, N., McKerrow, A., VanDriel, J.N., Wickham, J., 2007. Completion of the 2001 National Land Cover Database for the conterminous United States. Photogramm. Eng. Remote. Sens. 73, 337–341.

Scenarios Network for Alaska and Arctic Planning (SNAP), 2014. (Available at) http://www.snap.uaf.edu (accessed on Mar 6, 2014).

Hu, F.S., Higuera, P.E., Walsh, J.E., Chapman, W.L., Duffy, P.A., Brubaker, L.B., Chipman, M.L., 2010. Tundra burning in Alaska: linkages to climatic change and sea ice retreat. J. Geophys. Res. Biogeosci. 115, G04002. http://dx.doi.org/10.1029/2009JG001270.

Hugelius, G.H., Strauss, J., Zubrzycki, S., Kuhry, P., Harden, J.W., Schuur, E.A.G., Ping, C.-L., Schirrmeister, L., Michaelson, G., Harden, J.W., Koven, C.D., O'Donnel, J., Elberling, B., Mishra, U., Camill, P., Yu, Z., Palmtag, J., 2014. Estimated stocks of circumpolar permafrost carbon with quantified uncertainty ranges and identified data gaps. Biogeosciences 11, 6573–6593.

IPCC, 2013. Summary for policymakers. In: Stocker, T.F., Qin, D., Plattner, G.-K., Tignor, M., Allen, S.K., Boschung, J., Nauels, A., Xia, Y., Bex, V., Midgley, P.M. (Eds.), Climate Change 2013: the Physical Science Basis. Contribution of Working Group I to the Fifth Assessment Report of the Intergovernmental Panel on Climate Change. Cambridge University Press, Cambridge, United Kingdom and New York, NY, USA.

Jetz, W., Rahbek, C., Lichstein, J.W., 2005. Local and global approaches to spatial data analysis in ecology. Glob. Ecol. Biogeogr. 14, 97–98.

Ji, J., 1995. A climate-vegetation interaction model: Simulating physical and biological processes at the surface. J. Biogeogr. 22, 445–451.

Johnson, K.D., Harden, J., McGuire, A.D., Bliss, N.B., Bockheim, J.G., Clark, M., Nettleton-Hollingsworth, T., Jorgenson, M.T., Kane, E.S., Mack, M., O'Donnell, J., Ping, C., Schuur, E.A.G., Turetsky, M.R., Valentine, D.W., 2011. Soil carbon distribution in Alaska in relation to soil-forming factors. Geoderma 167, 71–84.

Jorgenson, M.T., Romanovsky, V., Harden, J.W., Shur, Y., O'Donnell, J., Schuur, E.A.G., Kanevskiy, M., Marchenko, S., 2010. Resilience and vulnerability of permafrost to climate change. Can. J. For. Res. 40, 1219–1236.

Karlstrom, T.N.V., 1964. Surficial geology of Alaska. U.S. Geological Survey, Washington, D.C. USGS Misc. Geol. Invest. Map I-357, 2 sheets, scale 1:1,584,000.

Koven, C.D., Ringeval, B., Friedlingstein, P., Ciais, P., Cadule, P., Khvorostyanov, D., Krinner, G., Tarnocai, C., 2011. Permafrost carbon-climate feedbacks accelerate global warming. Proc. Natl. Acad. Sci. U. S. A. 108, 14769–14774.

Koven, C.D., Riley, W.J., Stern, A., 2013a. Analysis of permafrost thermal dynamics and response to climate change in the CMIP5 earth system models. J. Clim. 26, 1877–1900.

Koven, C.D., Riley, W.J., Subin, Z.M., Tang, J.Y., Torn, M.S., Collins, W.D., Bonan, G.B., Lawrence, D.M., Swenson, S.C., 2013b. The effect of vertically resolved soil biogeochemistry and alternate soil C and N models on C dynamics of CLM4. Biogeosciences 10, 7109–7131.

Kutner, M.H., Nachtsheim, C.J., Neter, J., 2004. Applied Linear Regression Models. McGraw-Hill, New York.

Lawrence, D.M., Slater, A.G., 2005. A projection of severe near-surface permafrost degradation during the 21st century. Geophys. Res. Lett. 32, L24401. http://dx.doi.org/10.1029/2005GL025080.

MacDougall, A.H., Avis, C.A., Weaver, A.J., 2012. Significant existing commitment to warming from the permafrost carbon feedback. Nat. Geosci. 5, 719–721.

Malone, B.P., McBratney, A.B., Minasny, B., 2011. Empirical estimates of uncertainty for mapping continuous depth functions of soil attributes. Geoderma 160, 614–626.

Michaelson, G.J., Ping, C.L., Clark, M., 2013. Soil pedon carbon and nitrogen data for Alaska: an analysis and update. Open J. Soil Sci. 3, 132–142.

Minasny, B., McBratney, A.B., 2002. FuzME Version 3.0, Australian Centre for Precision Agriculture. The University of Sydney, Australia.

Minasny, B., McBratney, A.B., Malone, B.P., Wheeler, I., 2013. Digital mapping of soil carbon. Adv. Agron. 118, 1–47.

Mishra, U., Riley, W.J., 2012. Alaskan soil carbon stocks: spatial variability and environmental control. Biogeosciences 9, 3637–3645.

Mishra, U., Riley, W.J., 2014. Active-layer thickness across Alaska: comparing observation-based estimates with CMIP5 earth system model predictions. Soil Sci. Soc. Am. J. 78, 894–902.

Mishra, U., Riley, W.J., 2015. Scaling impacts on environmental controls and spatial heterogeneity of soil organic carbon stocks. Biogeosciences 12, 3993–4004.

Mishra, U., Lal, R., Liu, D., Van Meirvenne, M., 2010. Predicting the spatial variation of soil organic carbon pool at a regional scale. Soil Sci. Soc. Am. J. 74, 906–914.

Mishra, U., Jastrow, J.D., Matamala, R., Hugelius, G., Koven, C.D., Harden, J.W., Ping, C.L., Michaelson, G.J., Fan, Z., Miller, R.M., McGuire, A.D., Tarnocai, C., Kuhry, P., Riley, W.J., Schaefer, K., Schuur, E.A.G., Jorgenson, M.T., Hinzman, L.D., 2013. Empirical estimates to reduce modeling uncertainties of soil organic carbon in permafrost regions: a review of recent progress and remaining challenges. Environ. Res. Lett. 8, 035020. http://dx.doi.org/10.1088/1748-9326/8/3/035020.

Odeh, I.O.A., McBratney, A.B., Chittleborough, D.J., 1992. Soil pattern recognition with fuzzy-c-means: application to classification and soil landform interrelationships. Soil Sci. Soc. Am. J. 56, 505–516.

Pastick, N.J., Rigge, M., Wylie, B.K., Jorgenson, M.T., Rose, J.R., Johnson, K.D., Lei, J., 2014. Distribution and landscape controls of organic layer thickness and carbon within the Alaskan Yukon River Basin. Geoderma 230-231, 79–94.

Pau, G.S.H., Bisht, G., Riley, W.J., 2014. A reduced-order modeling approach to represent subgrid-scale hydrological dynamics for land-surface simulations: application in a polygonal tundra landscape. Geosci. Model Dev. 7, 2091–2105.

Ping, C.L., Bockheim, J.G., Kimble, J.M., Michaelson, G.J., Walker, D.A., 1998. Characteristics of cryogenic soils along a latitudinal transect in Arctic Alaska. J. Geophys. Res. 103, 28917–28928.

Ping, C.L., Michaelson, G.J., Jorgenson, M.T., Kimble, J.M., Epstein, H., Romanovsky, V.E., Walker, D.A., 2008. High stocks of soil organic carbon in the North American arctic region. Nat. Geosci. 1, 615–619.

Ping, C.L., Michaelson, G.J., Guo, L., Jorgenson, M.T., Kanevskiy, M., Shur, Y., Dou, F., Liang, J., 2011. Soil carbon and material fluxes across the eroding Alaska Beaufort Sea coastline. JGR-Biogeosci. 116, G02004. http://dx.doi.org/10.1029/2010jg001588.

Ping, C.L., Clark, M.H., Kimble, J.M., Michaelson, G.J., Shur, Y., Stiles, C.A., 2013. Sampling protocols for permafrost-affected soils. Soil Horiz. 54, 13–19.

Ping, C.L., Jastrow, J.D., Jorgenson, M.T., Michaelson, G.J., Shur, Y.L., 2015. Permafrost soils and carbon cycling. Soil 1, 147–171. http://dx.doi.org/10.5194/soil-1-147-2015.

Prince, S.D., Goward, S.J., 1995. Global primary production: a remote sensing approach. J. Biogeogr. 22, 316–336.

Reichstein, M., Bahn, M., Ciais, P., Frank, D., Mahecha, M.D., Seneviratne, S.I., Zscheischler, J., Beer, C., Buchmann, N., Frank, D.C., Papale, D., Rammig, A., Smith, P., Thonicke, K., van der Velde, M., Vicca, S., Walz, A., Wattenbach, M., 2013. Climate extremes and the carbon cycle. Nature 500, 287–295.

SAS Institute, 2011. Base SAS 9.3 Procedures Guide: SAS Institute, Inc. Cary, NC.

Schaefer, K., Zhang, T., Bruhwiler, L., Barrett, A.P., 2011. Amount and timing of permafrost carbon release in response to climate warming. Tellus B 63, 165–180.

Schirrmeister, L., Grosse, G., Wetterich, S., Overduin, P.P., Strauss, J., Schuur, E.A.G., Hubberten, H.-W., 2011. Fossil organic matter characteristics in permafrost deposits of the northeast Siberian Arctic. J. Geophys. Res. 116, G00M02. http://dx.doi.org/10.1029/2011jg001647.

Schneider von Deimling, T.S., Meinshausen, M., Levermann, A., Huber, V., Frieler, K., Lawrence, D.M., Brovkin, V., 2012. Estimating the near-surface permafrost-carbon feedback on global warming. Biogeosciences 9, 649–665.

Schuur, E.A.G., Abbott, B., 2011. High risk of permafrost thaw. Nature 480, 32–33.

Shrestha, D.L., Solomatine, D.P., 2006. Machine learning approaches for estimation of prediction interval for the model output. Neural Netw. 19, 225–235.

Soil Survey Staff, 2014. Keys to Soil Taxonomy. 12th ed. USDA-Natural Resources Conservation Service, Washington, DC.

Strauss, J., Schirrmeister, L., Wetterich, S., Borchers, A., Davydov, S.P., 2012. Grain-size properties and organic-carbon stock of Yedoma ice complex permafrost from the Kolyma lowland, northeastern Siberia. Glob. Biogeochem. Cycles 26, GB3003. http://dx.doi.org/10.1029/2011GB004104.

Takata, K., Emori, S., Watanabe, T., 2003. Development of the minimal advanced treatments of surface interaction and runoff. Glob. Planet. Chang. 38, 209–222.

Tarnocai, C., Stolbovoy, V., 2006. Northern peatlands: their characteristics, development and sensitivity to climate change. In: Martini, I.P., Martìnez Cortizas, A., Chesworth, W. (Eds.), Peatlands: Evolution and Records of Environmental and Climate Changes. Elsevier, Amsterdam, pp. 17–51.

Tarnocai, C., Canadell, J.P., Schuur, E.A.G., Kuhry, P., Mazhitova, G., Zimov, S., 2009. Soil organic carbon pools in the north circumpolar permafrost region. Glob. Biogeochem. Cycles 23, GB203. http://dx.doi.org/10.1029/2008GB003327.

Taylor, K. E., Stouffer, R.J., Meehl, G.A., 2009. A summary of the CMIP5 experiment design. PCMDI Tech. Rep., 33 pp. [Available online at http://cmip-pcmdi.llnl.gov/cmip5/docs/Taylor_CMIP5_design.pdf]

Circumpolar Active Layer Monitoring Network (CALM), 2013. The circumpolar active layer thickness data. (available at) http://www.gwu.edu/~calm/data/north.html (accessed 24 Jan 2013).

Thompson, J.A., Pena-Yewtukhiw, E.M., Grove, J.H., 2006. Soil–landscape modeling across a physiographic region: topographic patterns and model transportability. Geoderma 133, 57–70.

Todd-Brown, K.E.O., Randerson, J.T., Post, W.M., Hoffman, F.M., Tarnocai, C., Schuur, E.A.G., Allison, S.D., 2013. Causes of variation in soil carbon predictions from CMIP5 Earth system models and comparison with observations. Biogeosciences 10, 1717–1736.

Verseghy, D.L., 1991. CLASS—A Canadian land surface scheme for GCMS. I. Soil model. Int. J. Climatol. 11, 111–133.

Wieder, W.R., Bonan, G.B., Allison, S.D., 2013. Global soil carbon projections are improved by modeling microbial processes. Nat. Clim. Chang. 3, 909–912.

Zhang, Y., Chen, W., Smith, S.L., Riseborough, D.W., Cihlar, J., 2005. Soil temperature in Canada during the twentieth century: complex responses to the changes in air temperature at high latitudes. J. Geophys. Res. 110, D03112. http://dx.doi.org/10.1029/2004JD004910.

Zhang, C., Tang, Y., Xu, X., Kiely, G., 2011. Towards spatial geochemical modelling: Use of geographically weighted regression for mapping soil organic carbon contents in Ireland. Appl. Geochem. 26, 1239–1248.